Proceedings of the 21st ICSMGE, Vienna, Austria, 14 – 19 June 2026. Pistrol, Adam & Schweiger (eds.)
Published by: ÖGG, Austrian Society for Geomechanics, Salzburg, Austria, ISBN 978-3-9503898-4-5
https://doi.org/10.53243/ICSMGE2026-1006

Directional Shear Resistance of Snakeskin-inspired Pile Under Monotonic Loading

Tae-Young Kim and Song-Hun Chong
Department of Civil Engineering, Sunchon National University, Republic of Korea, shchong@scnu.ac.kr

ABSTRACT: Bio-inspired designs based on snake ventral scales have attracted increasing attention for their capability to select shear resistance developed through directional frictional anisotropy. This study investigates the shear resistance anisotropy of snakeskin-inspired pile under penetration-pullout loading sequences in sand. A series of small-scale cone tests are conducted in a soil chamber. Results show that bio-inspired piles consistently increase the measured cone loads compared to smooth piles, with the cranial direction (against the scales) producing greater resistance than the caudal direction (along the scales) in all cases. Enhanced surface roughness, characterized by higher scale heights or shorter scale lengths, amplifies the cone load during both penetration and pullout. Further analysis indicates that the normalized cone load increases with a greater scale ratio (H/L), converging to asymptotic values at larger H/L ratios. These findings highlight the potential of bio-inspired piles for optimizing load transfer mechanisms in geotechnical applications by leveraging directional shear resistance.

KEYWORDS: Bio-inspired designs, snakeskin-inspired piles, small-scale cone tests, directional shear resistance.

1 INTRODUCTION

Recently, bio-inspired geotechnics offers innovative solutions by mimicking nature's evolutionary designs (Ghazlan et al. 2020; Mallett et al. 2018; Zhang et al. 2023). A representative geotechnical application is inspired by snake skin whose anisotropic surface structure enables efficient locomotion through directional friction control. Snakes possess specialized ventral scales that produce a sawtooth pattern, enhancing resistance in one direction while minimizing resistance in the other. These frictional properties have inspired surface modifications to selectively utilize the interaction between soil and geo-structures. For instance, deep foundations and soil nailing subjected to axial loads require larger mobilized shear resistance for effective load transfer, while minimal shear resistance is desirable in applications such as pile driving and soil sampling (Hazel et al. 1999; Martinez et al. 2019; O'Hara & Martinez 2020; Stutz & Martinez 2021; Zhong et al. 2021). Previous studies have revealed that interface frictional anisotropy is affected by loading direction, surface roughness, and soil characteristics. Cranial shearing (movement against the ventral scales) mobilized greater peak and residual interface strength, as well as dilation, compared to caudal shearing (movement along the scales). This is because cranial shearing caused more significant soil deformations and dilation. This movement allows soil particles to latch onto the ventral scales, increasing the contact area and generating wedges in front of the scales, where shear and volumetric strains are localized. These wedges led to an increase in local effective stress. Conversely, caudal shearing prevented the soil from latching onto the scales, reducing the contact area and resulting in less deformation (Lee et al. 2023; Nawaz et al. 2024; O'Hara & Martinez 2024). In addition, a series of centrifuge cone penetration tests were conducted to explore the load transfer mechanism across bio-inspired pile. Unique frictional anisotropy was observed during both penetration and pullout: bio-inspired surfaces can reduce friction during penetration while increasing pullout resistance, providing a potential solution for deep foundation applications (Martinez & O'Hara 2021; O'Hara & Martinez 2022). However, there remains a need to quantitatively estimate pile resistance with various snake-inspired surfaces under different loading directions. This study aims to evaluate the shear resistance anisotropy of bioinspired piles under loading direction (penetration → pullout) using a small-scale bioinspired cone and cone penetration apparatus. A total of 11 cone penetration tests are performed in sand using five bioinspired cones and a reference smooth cone under both loading directions (penetration → pullout) at constant vertical stress condition. Further analysis is conducted to summarize the normalized cone resistance as a function of surface scale geometry and loading direction.

2 EXPERIMENTAL STUDY

2.1 *Development of cone penetration test apparatus*

For the characterization of the direction-dependent shear resistance behavior of snakeskin-inspired piles, a small-scale cone penetration apparatus was developed (Kim et al., 2024). The apparatus consists of a soil chamber, loading system, reaction frames, cone control system, and data acquisition system. The soil chamber is a square container with internal dimensions of 700 × 700 × 700 mm and a wall thickness of 50 mm to maintain a zero lateral strain condition. Vertical stress is applied using a 40 mm-thick square steel plate (695 × 695 mm), and its magnitude is calculated by dividing the applied force by the plate's cross-sectional area. The reaction frame plays a crucial role in withstanding the forces generated during cone penetration, supporting the vertical actuator, and providing space for both penetration and pullout operations. A cone penetration rate of 10 mm/sec is applied, with cone resistance measured by a load cell attached to the pile head, while vertical displacement is monitored using a wire-type displacement transducer fixed to the actuator housing. All data are collected at a sampling rate of 2 Hz, and all sensors are connected to the data acquisition system.

2.2 *Soil properties*

Jumunjin sand is a poorly graded, sub-rounded silica sand (SiO_2 = 88.21%), with a specific gravity (G_s) of 2.62, median grain size (D_{50}) of 0.58 mm, a coefficient of uniformity (C_U) of 1.46, a coefficient of curvature (C_C) of 0.93, a maximum void ratio (e_{max}) of 0.92, and a minimum void ratio (e_{min}) of 0.62.

2.3 *Small-scale piles with snakeskin-inspired shaft*

In this study, five bio-inspired cones and a smooth reference cone are tested under both loading directions (penetration → pullout). Figure 1 shows the textured cone inspired by the snake's ventral surface and summarizes the different combinations of scale geometries in Table 1. All cones are made of durable stainless steel (diameter of 14 mm, length of 483 mm, and a conical tip with a 60° apex angle) and consist of three sections (the upper, middle, and lower parts). The upper section, 260 mm in length, is connects to the hollow load cell. A middle section of 180 mm length, featuring a surface asperity with varying length and height, designed to change of the

asperity orientation. The lower section is 30 mm length with a smooth surface and a 13 mm conical tip. There are no strain gauges installed within cone tip. Note that the measured force is a combination of skin friction and tip resistance during penetration while the skin friction along the cone shaft is only measured during pullout.

2.4 *Test program*

The soil model is compacted by dividing seven layers to a uniform target relative density equal to 64% using Jumunjin sand. The volume of the prepared soil model is identical to the internal volume of the chamber. The sand is spread in the container and each sublayer is compacted using a 2.5 kg circular steel tamping rod with a diameter of 50 mm. This steel tamping rod is dropped 100 times from a height of approximately 300 mm for every sublayer. This process is repeated seven times to model the soil sample.

A total of 11 cone load tests are performed on five bio-inspired cones and a reference smooth cone under both loading directions (penetration to pullout) at a vertical stress of 100 kPa. Prior to cone penetration, vertical stress is applied to the soil sample. Subsequently, the cones are penetrated to a target depth of 300 mm, followed by a 50 mm pullout test. The cone penetration rate is maintained at a 10 mm/sec during the cone tests. The cone load values during penetration process are defined by taking average value between depths of 50 and 200 mm for cone penetration load while the cone pullout load value is the average value between depths of 300 and 250 mm.

Table 1. Geometry of snakeskin-inspired piles. Note that test designation 'CD-CR' represents caudal first penetration and cranial second pullout sequence, while 'CR-CD' means cranial first penetration and caudal second pullout sequence.

Test designation	Scale geometry [mm]		Scale ratio, H/L [-]
	Length, L	Height, H	
CD-CR1	20	0.3	0.015
CR-CD1	20	0.3	0.015
CD-CR2	20	0.5	0.025
CR-CD2	20	0.5	0.025
CD-CR3	6	0.3	0.05
CR-CD3	6	0.3	0.05
CD-CR4	60	4	0.067
CR-CD4	60	4	0.067
CD-CR5	20	4	0.2
CR-CD5	20	4	0.2
Smooth	-	-	-

3 RESULTS

Figure 2 shows the change in normalized cone load for both the smooth and bio-inspired cones over the entire test duration. The normalized load is calculated by dividing the measured cone force by vertical load (= 25 kN). Note that the positive sign convention of the normalized load indicates the penetration test. Regardless of the presence of surface asperities, the cone resistance shows minimal variation during the initial penetration phase, but steadily increases afterward. After 8 seconds of penetration, the bio-inspired cone (caudal to cranial test) produces a higher cone load compared to the smooth cone, with the maximum normalized load of the bio-inspired cone (= 0.14) being higher than that of the smooth cone (= 0.09). During the pullout phase (30 seconds after the cone tests), the bio-inspired cone initially exhibits a higher pullout normalized load and reaching a maximum pullout load (= -0.038) at 33 seconds and then gradually decreasing. In contrast, smooth cone shows constant pullout normalized load (= -0.015).

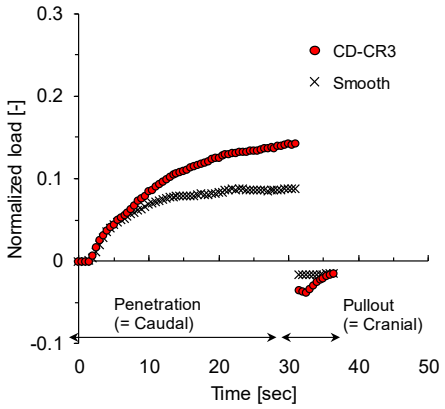

Figure 2. Time series for penetration and pullout test sequence.

Figure 3 shows the variation in normalized load as a function of surface asperity geometry (scale height and scale length) and loading direction. Each result presents the normalized load and normalized depth, where the normalized depth is determined by dividing the penetration depth of the cone by the total soil model depth (= 700 mm). Similar load transfer trends are observed in all cases; the normalized load is minimal near the specimen surface. Thereafter, the penetration load continuously increases, and after reaching critical depth, the ultimate normalized load is observed. However, the normalized cone load suddenly decreases during the pullout process. In particular, larger normalized loads are measured on the bio-inspired cones, and the cranial first penetration direction produces a larger normalized load compared to the caudal first penetration direction.

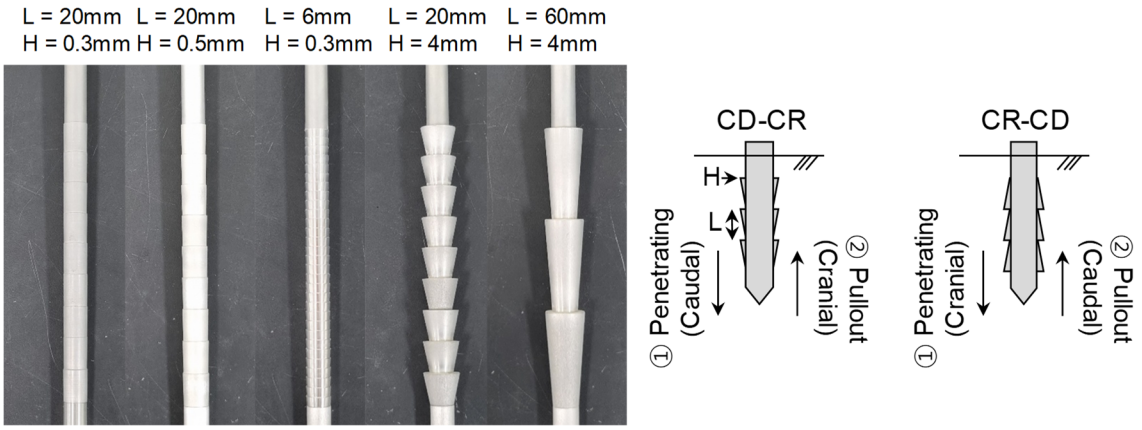

Figure 1. Geometry of textured piles used in this study. The parameter L represents the scale length and H is the scale height. The total length of the surface scale remains constant at 180 mm across all piles.

An increased scale height leads to greater shear resistance along the cone, ultimately resulting in a higher normalized cone load in both penetration-pullout sequences (i.e., cranial to caudal and caudal to cranial tests), as shown in Figures 3(a) and (b). In contrast, a reduced scale length generates a higher normalized cone load during both the cranial to caudal and caudal to cranial tests, as illustrated in Figures 3(c) and (d). Surfaces with shorter scale length contain more scales, contributing to a higher normalized cone load. This effect arises because a larger scale height or a greater number of scales (i.e., shorter scale length) increases the surface roughness, which facilitates the formation of lager passive wedges, causing dilation of the soil ahead of the scales and contraction behind them, as observed in prior interface direct shear test (Martinez et al. 2019).

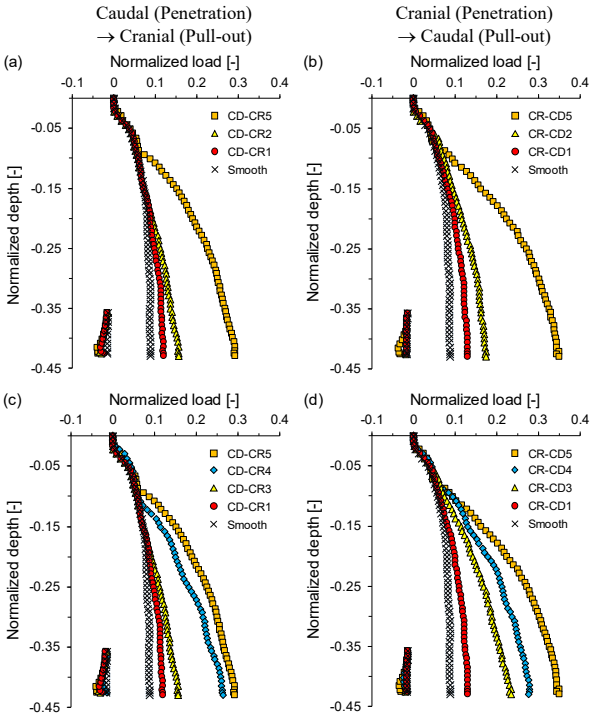

Figure 3. Effect of surface asperity on measured load for two loading directions: (a and b) scale height (L = 20 mm fixed); (c and d) scale length (H = 0.3 and 4 mm fixed).

Figure 4 presents the response of normalized cone resistance as a function of normalized pullout displacement following the penetration test. The normalized pullout displacement is obtained by dividing the pullout depth by the total cone length (= 483 mm). The pullout load of the smooth cone remains nearly constant, while the bio-inspired cones generate higher pullout loads. A larger scale height [Figures 4(a) and (b)] or shorter scale length [Figures 4(c) and (d)] results in a greater normalized pullout load. A strain-hardening response is observed, where the normalized pullout load increases dramatically up to a certain normalized displacement. After reaching the maximum pullout load, it gradually decreases and eventually stabilizes at the critical force, regardless of scale geometry and loading direction. As expected, the cranial pullout direction consistently produces a larger normalized pullout load compared to the caudal pullout direction in all cases.

4 DISCUSSION

In the previous sections, the cone load is explored through various scale geometries and two loading directions. Furthermore, the scale geometry ratio, defined as the ratio of scale height to length (H/L), is used to analyze the shear resistance between sand and bio-inspired cones. Figure 5 shows the normalized cone load as a function of H/L ratio. Note that the normalized cone load is defined by dividing the difference of cone force between the penetration and pullout tests by the applied load. Compared to the smooth cone, the bio-inspired cone produces a higher normalized cone load at all scale geometry ratio regardless of loading direction. The normalized cone load mobilized from the cranial first penetration direction is larger than caudal first penetration, as penetration measurements obtained the cone tip and skin resistance, while the pullout tests reflect only skin resistance. The normalized cone load between the cranial first direction and the caudal first direction varies from 0.104 to 0.196 for caudal to cranial and 0.109 to 0.215 for cranial to caudal. The normalized cone load significantly increases until H/L = 0.07, followed by a gradual increase between H/L = 0.07 to H/L = 0.2 in the cranial and caudal directions. The scales of the surfaces with a small H/L form shear bands with more uniform soil deformation, while a higher H/L mobilizes the interface soil resistance developed by a well-defined passive wedge (Martinez et al., 2019). In particular, the difference in normalized cone load between both penetration-pullout sequence (i.e., cranial to caudal and caudal to cranial tests) gradually increases from 0.005 at H/L = 0.015 to 0.02 at H/L = 0.2.

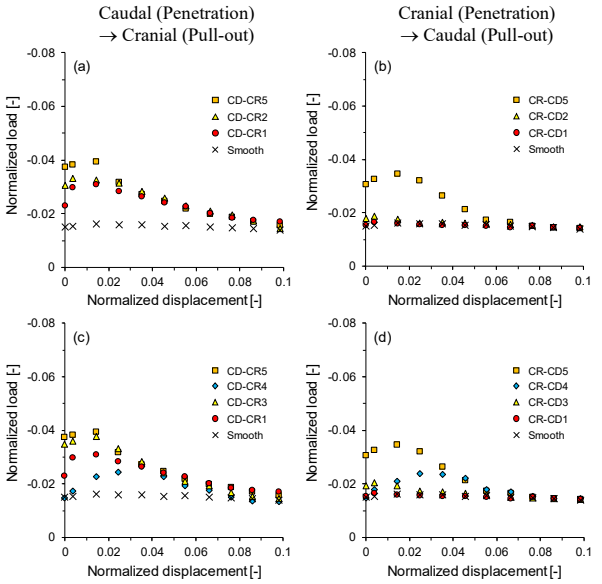

Figure 4. Change of measured pullout force after penetration test: (a and b) scale height (L = 20 mm fixed); (c and d) scale length (H = 0.3 and 4 mm fixed).

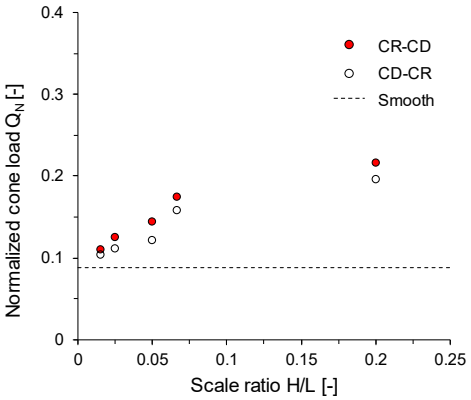

Figure 5. Change in normalized pile load as a function of scale ratio (H/L).

5 CONCLUSIONS

In this study, a small-scale cone apparatus is developed to quantitatively evaluate the loading direction-dependent shear resistance of textured cones with snakeskin bio-inspired asperity. The salient conclusions are drawn as follows:

- Comparing the smooth cone, the bio-inspired cones produce a greater normalized cone load irrespective of asperity orientation (i.e., cranial to caudal and caudal to cranial tests) in all cases. In addition, the cranial direction mobilizes a larger normalized cone load than caudal direction, regardless of loading directions.
- At a given scale geometry, a higher scale height or shorter scale length produce a larger normalized cone load in both penetration-pullout sequences. A higher scale height indicates a rough surface that induces passive wedges around the scales, increasing the cone load. Meanwhile, shorter scales correspond to a greater number of scales, producing a higher normalized cone load.
- A strain-hardening response is observed, with pullout load peaking and then gradually decreasing to a critical cone load. Cranial pullout consistently results in higher resistance than caudal pullout.
- The normalized cone load as function of scale geometry ratio (H/L) helps to understand the interface anisotropy response. A greater H/L ratio mobilize a higher normalized cone load, with a significant increase up to H/L = 0.07, whereas surfaces with smaller H/L ratios tend to have a lower normalized cone load.

6 ACKNOWLEDGEMENTS

This work was supported by the National Research Foundation of Korea (NRF) grant funded by the Korea government (No. RS-2025-25412264)

7 REFERENCES

Ghazlan, A., Ngo, T., Tran, P., Le, V.T., Nguyen, T., Whittaker, A.S., and Remennikov, A. 2020. Enhancing toughness of medium-density fiberboard by mimicking nacreous structures through advanced manufacturing techniques. *Journal of Structural Engineering* 146(3), 04020001.

Hazel, J., Stone, M., Grace, M., and Tsukruk, V. 1999. Nanoscale design of snake skin for reptation locomotions via friction anisotropy. *Journal of biomechanics* 32(5), 477-484.

Kim, T.Y., Jung, K.H., and Chong, S.H. 2024. Development of a cone penetration testing apparatus with a textured shaft. *Applied Sciences* 14(22), 10090.

Lee, S.H., Nawaz, M.N., and Chong, S.H. 2023. Estimation of interface frictional anisotropy between sand and snakeskin-inspired surfaces. *Scientific Reports* 13(1), 3975.

Mallett, S., Matsumura, S., and David Frost, J. 2018. Additive manufacturing and computed tomography of bio-inspired anchorage systems. *Géotechnique Letters* 8(3), 219-225.

Martinez, A., and O'Hara, K. 2021. Skin friction directionality in monotonically-and cyclically-loaded bio-inspired piles in sand. *Deep Foundations Institute Journal* 15(1), 1-15.

Martinez, A., Palumbo, S., and Todd, B.D. 2019. Bioinspiration for anisotropic load transfer at soil–structure interfaces. *Journal of Geotechnical and Geoenvironmental Engineering* 145(10), 04019074.

Nawaz, M. N., Lee, S.-H., Chong, S.-H., and Ku, T. 2024. Interface frictional anisotropy of dilative sand. *Scientific Reports* 14(1), 6166.

O'Hara, K.B., and Martinez, A. 2024. Direction-dependent failure envelopes of sand-structure interfaces with snakeskin-inspired surfaces. *Canadian Geotechnical Journal* 61(12), 2755-2773.

O'Hara, K.B., and Martinez, A. 2020. Monotonic and cyclic frictional resistance directionality in snakeskin-inspired surfaces and piles. *Journal of Geotechnical and Geoenvironmental Engineering* 146(11), 04020116.

O'Hara, K.B., and Martinez, A. 2022. Load transfer directionality of snakeskin-inspired piles during installation and pullout in sands. Journal of Geotechnical and Geoenvironmental Engineering, 148(12), 04022110.

Stutz, H.H., and Martinez, A. 2021. Directionally dependent strength and dilatancy behavior of soil–structure interfaces. *Acta Geotechnica* 16(9), 2805-2820.

Zhang, N., Chen, Y., Martinez, A., and Fuentes, R. 2023. A bioinspired self-burrowing probe in shallow granular materials. *Journal of Geotechnical and Geoenvironmental Engineering* 149(9), 04023073.

Zhong, W., Liu, H., Wang, Q., Zhang, W., Li, Y., Ding, X., and Chen, L. 2021. Investigation of the penetration characteristics of snake skin-inspired pile using DEM. *Acta geotechnica* 16, 1849-1865.